

# Sidelobe Suppression for Non-systematic Coded UW-OFDM in Cognitive Radio Networks

Morteza Rajabzadeh<sup>\*†</sup>, Hossein Khoshbin<sup>†</sup>, Heidi Steendam<sup>\*</sup>

<sup>\*</sup>DIGCOM Research Group, TELIN Dept., Ghent University, Ghent, Belgium

<sup>†</sup>Electrical Engineering Department, Ferdowsi University of Mashhad, Mashhad, Iran

**Abstract**—In this paper, a novel non-contiguous non-systematic coded unique word (UW)-OFDM system is proposed to opportunistically transmit data on the spectrum holes available in a cognitive radio network. In such a system, the spectral sidelobes of the active subcarriers interfere with the adjacent spectral band used by the primary system. In the proposed scheme, the code generator matrix of the UW-OFDM is designed to suppress the sidelobes. So, there is no need to add any extra processing to the transmitter for suppressing sidelobes. The derived code generator matrix is optimum in the sense of being matched to the best linear unbiased estimator and to the linear minimum mean square error data estimators. The achieved sidelobe suppression is a function of the number of transmitted data symbols. Simulation results show that by a slight decrease in the number of transmitted data symbols, the sidelobes power can be suppressed to zero.

**Index Terms**—unique word OFDM; sidelobe suppression; cognitive radios; code generator matrix.

## I. INTRODUCTION

The increased demand for bandwidth in wireless communication and under-utilization of the available spectrum [1] make the efficient use of the radio spectrum very important. To this aim, cognitive radio (CR) technology has been introduced to exploit the spectrum opportunistically [2]. After spectrum sensing and determining the available spectrum, the CR user is allowed to use parts of the spectrum that are not used by the primary system while keeping the spectral interference to the spectral band used by the primary system below a tolerable level. The spectral shape of the transmitted signal needs to be highly flexible so as to dynamically adapt to the environment.

Multicarrier techniques, especially cyclic prefix (CP)-OFDM, are considered as the favorite air-interface technology for CR networks because by dividing a frequency band into orthogonal subcarriers, they have the flexibility to fill the spectrum gaps and utilize non-adjacent spectrum bands with variable widths [3]. However, conventional CP-OFDM signals exhibit relatively high spectral sidelobes power, which may impose interference to the primary users operating in adjacent bands. Consequently, much study is devoted to find efficient sidelobe suppression approaches for CP-OFDM systems. For example, in active interference cancellation (AIC) [4] and cancellation carrier (CC) [5] approaches, a number of subcarriers residing in the vicinity of the primary band are used to suppress the sidelobes. However, a considerable part of OFDM symbol energy should be allocated to them resulting in degraded bit error rate (BER) performance. The achieved sidelobe suppression by adaptive symbol transition

(AST) [6], constellation expansion (CE) [7] and active point modification (APM) [8] are not very high. Moreover, these approaches either reduce the data rate or decrease the system error performance. To overcome the drawbacks of the former techniques, other solutions were proposed. For example, a sidelobe suppression of about 70 dB was reported when using antipodal subcarrier coding scheme [9]. Also precoding schemes were proposed for CP-OFDM systems to lower the sidelobes [10]. The precoders proposed in [11], [12] are able to achieve a suppression of the order of 100 dB. Although these precoders achieve satisfactory sidelobe suppression levels, they introduce distortions to the transmitted data symbols resulting in degraded BER performance. Moreover, the family of spectral precoders for sidelobe suppression incurs additional complexity at both the transmitter and the receiver.

Recently, a new multicarrier technique known as UW-OFDM is introduced [13] in which in contrast to other guard interval based multicarrier techniques, the guard interval is part of inverse discrete Fourier transform (IDFT), i.e., the last samples of the IDFT block do not contain a data contribution but exist of known samples—the unique word. This requires the introduction of redundancy in the frequency domain. In the non-systematic coded UW-OFDM, proposed in [14], the redundancy is distributed over all active subcarriers by using a code generator matrix. UW-OFDM has shown good data transmission performances, which makes it a promising multicarrier transmission scheme for future high data rate communication. In [13], [14], [15], it is shown that UW-OFDM outperforms CP-OFDM in frequency selective fading channels in the sense of BER. This is because of the inherent redundancy in the frequency domain, which introduces a coding gain in UW-OFDM as compared to CP-OFDM. The price to be paid is the need of more complex data estimators [16]. However, when the channel coding is used at the transceiver on top of the modulation, this difference in complexity will diminish because the turbo decoder has much higher complexity than the data estimator. The throughput efficiency of UW-OFDM is investigated in [17], and it is shown that under the same communication settings, the throughput efficiency of UW-OFDM is just slightly lower than that of CP-OFDM.

Another important advantage of UW-OFDM is that out-of-band (OOB) radiation of UW-OFDM is lower than the OOB radiation of CP-OFDM [14], [18]. Inspired by this characteristics, we propose in this paper to use a non-systematic coded UW-OFDM as the physical layer of a cognitive radio

system which is allowed to transmit data in the non-contiguous parts of the spectrum that are not used by the primary system. First of all, it will be shown that simply turning-off the UW-OFDM subcarriers located in the primary system band results in lower sidelobes compared to doing this process (turning-off the subcarriers) for CP-OFDM. This is one of the advantages of UW-OFDM over CP-OFDM for being utilized as the physical layer technique in cognitive radios. Furthermore, we look in this paper at the effect of the code generator matrix on the sidelobes power. The main functionality of the code generator matrix is to spread the required redundancy over all subcarriers. Moreover, in [14], the code generator matrix is optimally designed to be matched to the best linear unbiased estimator (BLUE) and to the linear minimum mean square error (LMMSE) data estimators. In this paper, while keeping the above mentioned functionalities for the code generator matrix, it is further designed to suppress the sidelobes power leaked to the adjacent band used by the primary system when UW-OFDM is used as the physical layer technique of the cognitive radio. To find the optimal code generator matrix, the leaked spectral sidelobes power to the adjacent primary band is considered as the cost function to be minimized, and the code generator matrix is the variable matrix that should be designed by solving this minimization problem. Based on the derivations in [14], suitable constraints are added to the minimization problem so that the derived code generator matrix is matched to the BLUE and the LMMSE data estimators. It is shown by simulations that the proposed UW-OFDM system with sidelobe suppression (SLS-UW) is able to suppress the sidelobes by more than 160 dB, which is almost zero. This is far better than the level of sidelobe suppression achieved by most of the proposed sidelobe suppression approaches for the CP-OFDM transmission scheme. In the simulation results, it is shown that this good sidelobe suppression performance can be achieved by slightly decreasing the number of transmitted data symbols. However, a compromise can be made between the desired level of sidelobe suppression and the reduction of the number of transmitted data symbols. Another advantage of the proposed scheme is that it does not need extra processing to be added to the transmitter.

**Notations:** Vectors are indicated with bold lower-case letters. Matrices are indicated with bold capital letters. Super-scripts  $\{\}^T$ ,  $\{\}^H$ ,  $\{\}^{-1}$  represent transpose, Hermitian and inversion, respectively. The notations  $E\{\}$  and  $\text{Tr}[\ ]$  represent the expectation and trace operators, respectively. Notation  $\mathbf{0}_{M \times N}$  indicates the  $M \times N$  matrix with all-zero entries, while  $\mathbf{I}_M$  stands for the  $M \times M$  identity matrix.

## II. SYSTEM MODEL

For generating the data sequence of the non-systematic coded UW-OFDM, the two-step approach is used [13]. The output of the  $N$ -IDFT block in the transmitter is a block of  $N$  time-domain samples characterized by  $\mathbf{x} = [\mathbf{x}_d^T \ \mathbf{x}_u^T]^T$  in which the first  $N - N_u$  samples,  $\mathbf{x}_d \in \mathbb{C}^{N_d \times 1}$ , are random and depend on the data and the last  $N_u$  samples,  $\mathbf{x}_u \in \mathbb{C}^{N_u \times 1}$ , contain the known sequence which is called unique word. To

be able to add the unique word, in the first step, a block of  $N_u$  zeroes in the time domain is generated. In the systematic coded implementation of UW-OFDM systems, this is achieved by replacing  $N_r$  data carriers by redundant carriers, where  $N_r \geq N_u$ . The problem in systematic UW-OFDM is that the energy required for the redundant symbols is quite high [19].

In order to lower the energy required for the redundant symbols, the authors of [14] proposed to spread the redundant energy on all the subcarriers. This is done by using a precoder matrix,  $\mathbf{G} \in \mathbb{C}^{(N_d+N_r) \times N_d}$ , which can also be considered as a code generator matrix. Consider  $\tilde{\mathbf{d}} \in \mathbb{C}^{N_d \times 1}$  as the vector of  $N_d$  modulated data symbols that are independently and identically distributed ( $E\{\tilde{\mathbf{d}}\tilde{\mathbf{d}}^H\} = \mathbf{I}_{N_d}$ ) with zero mean ( $E\{\tilde{\mathbf{d}}\} = \mathbf{0}_{N_d \times 1}$ ). After the  $N_{dr} = N_d + N_r$  data and redundant carriers are distributed on the available subcarriers by multiplying  $\mathbf{G}$  and  $\tilde{\mathbf{d}}$ , similarly as in conventional OFDM systems,  $N_z = N - N_{dr}$  zero subcarriers are inserted at DC and band edges. So, the frequency domain data vector is given by

$$\tilde{\mathbf{x}} = \mathbf{B}\mathbf{G}\tilde{\mathbf{d}}, \quad (1)$$

where  $\mathbf{B} \in \mathbb{R}^{N \times (N_d+N_r)}$  inserts the zero subcarriers. Compared to the systematic coded UW-OFDM implementation, the original data symbols,  $\tilde{\mathbf{d}}$ , do not appear after being multiplied with  $\mathbf{G}$ . Therefore, this implementation of UW-OFDM systems is called non-systematic coded UW-OFDM [14]. The precoder matrix,  $\mathbf{G}$ , distributes the energy of the  $N_d$  symbols on all the active subcarriers. It also introduces the redundancy which is used to generate the required zeros at the output of the IDFT:

$$\mathbf{x}' = \mathbf{F}_N^{-1}\mathbf{B}\mathbf{G}\tilde{\mathbf{d}} = \begin{bmatrix} \mathbf{x}_d \\ \mathbf{0}_{N_u \times 1} \end{bmatrix}, \quad (2)$$

where  $\mathbf{x}'$  is  $N \times 1$  and  $\mathbf{x}_d$  is  $(N - N_u) \times 1$ . In other words, every column vector of  $\mathbf{G}$  must be orthogonal to the  $N_u$  lowermost row vectors of  $\mathbf{F}_N^{-1}\mathbf{B}$ . Until now, the generation of  $N_u$  zeros in the time-domain data vector is discussed. The next step is to insert the desired unique word vector,  $\mathbf{x}_u \in \mathbb{C}^{N_u \times 1}$ , instead of zeros, as follows:

$$\mathbf{x} = \mathbf{x}' + \begin{bmatrix} \mathbf{0} \\ \mathbf{x}_u \end{bmatrix} = \begin{bmatrix} \mathbf{x}_d \\ \mathbf{x}_u \end{bmatrix}, \quad (3)$$

The unique word vector,  $\mathbf{x}_u$ , is selected based on the requirements of the transmitter/receiver [13].

## III. SIDELOBE SUPPRESSION BY CODE GENERATOR MATRIX DESIGN

Assume the cognitive radio system detects the signal of a primary user transmitted in the part of the spectrum corresponding to  $N_n$  subcarriers with indices  $\Gamma_n = \{\sigma_1, \sigma_1 + 1, \dots, \sigma_2\}$ . The cognitive radio system employing the UW-OFDM transmission scheme should create spectral notches at this band. Therefore, we first characterize the spectrum of the UW-OFDM and determine the power leaked to the notch band.

### A. The leaked power to the notch band

Consider the time-domain data vector at the  $l$ th data block to be  $\mathbf{x}^{(l)}$ . In order to model the leaked power to the notch band and to have a good resolution of the spectrum of the UW-OFDM system, we upsample the subcarrier spacing by a factor  $N_s$ . The  $N_s$ -upsampled in-band frequency response of the UW-OFDM system can be characterized as follows [4]:

$$y_i^{(l)} = \sum_{n=0}^{N-1} x_n^{(l)} e^{-j2\pi n \frac{i}{N_s N}}, \quad i = 0, 1, \dots, N_s N - 1. \quad (4)$$

The  $N_s$ -upsampled spectral samples are accumulated in an  $N_s N \times 1$  vector as follows:

$$\mathbf{y}^{(l)} = \mathbf{E} \mathbf{x}^{(l)} = \mathbf{E} \mathbf{F}_N^{-1} \mathbf{B} \mathbf{G} \tilde{\mathbf{d}}^{(l)}, \quad (5)$$

where  $\mathbf{E}$  is the  $N_s N \times N$  upsampled Fourier matrix with  $(i, n)$ th entry  $[\mathbf{E}]_{i,n} = e^{-j2\pi n \frac{i}{N_s N}}$ .

Let us define the subset of indices of the upsampled spectrum located within the notch band as  $\Gamma_n^{UP} = \{N_s \sigma_1, N_s \sigma_1 + 1, \dots, N_s \sigma_2\}$ . A subset of  $\mathbf{E}$  is formed as  $\mathbf{E}_n$  which contains only those rows of  $\mathbf{E}$  whose indices are in the set  $\Gamma_n^{UP}$ , arranged in their natural order. Therefore, the upsampled frequency response of the cognitive radio transmitter at the notch band can be determined by using  $\mathbf{E}_n$  instead of  $\mathbf{E}$  in (5). Because the data vector  $\tilde{\mathbf{d}}^{(l)}$  is composed of random processes, the samples  $y_i^{(l)}$  are also random processes. Hence, the average leaked power to the notch band can be defined as

$$P_n = E \left\{ \|\mathbf{E}_n \mathbf{F}_N^{-1} \mathbf{B} \mathbf{G} \tilde{\mathbf{d}}^{(l)}\|_2^2 \right\} \quad (6)$$

in which  $\|\cdot\|_2$  denotes the 2-norm operator. The leaked power,  $P_n$ , can be rewritten as

$$P_n = E \left\{ \tilde{\mathbf{d}}^{(l)H} \mathbf{G}^H \mathbf{B}^H \mathbf{F}_N \mathbf{E}_n^H \mathbf{E}_n \mathbf{F}_N^{-1} \mathbf{B} \mathbf{G} \tilde{\mathbf{d}}^{(l)} \right\} \quad (7)$$

Now, we convert (7) to a form that is suitable for the design of our sidelobe suppression algorithm. The relation (7) can be expressed by the trace operator as follows:

$$P_n = E \left\{ \text{Tr} \left[ \mathbf{E}_n \mathbf{F}_N^{-1} \mathbf{B} \mathbf{G} \tilde{\mathbf{d}}^{(l)} \tilde{\mathbf{d}}^{(l)H} \mathbf{G}^H \mathbf{B}^H \mathbf{F}_N \mathbf{E}_n^H \right] \right\}. \quad (8)$$

Both the expectation and trace operators are linear, hence, they can be swapped and (8) becomes

$$\begin{aligned} P_n &= \text{Tr} \left[ \mathbf{E}_n \mathbf{F}_N^{-1} \mathbf{B} \mathbf{G} E \left\{ \tilde{\mathbf{d}}^{(l)} \tilde{\mathbf{d}}^{(l)H} \right\} \mathbf{G}^H \mathbf{B}^H \mathbf{F}_N \mathbf{E}_n^H \right] \\ &= \text{Tr} \left[ \mathbf{E}_n \mathbf{F}_N^{-1} \mathbf{B} \mathbf{G} \mathbf{G}^H \mathbf{B}^H \mathbf{F}_N \mathbf{E}_n^H \right]. \end{aligned} \quad (9)$$

Applying the fact that  $\text{Tr}[\mathbf{J}\mathbf{Q}] = \text{Tr}[\mathbf{Q}\mathbf{J}]$  to (9), the leaked power to the notch band is converted to

$$P_n = \text{Tr}[\mathbf{G}^H \mathbf{A} \mathbf{G}], \quad (10)$$

where  $\mathbf{A} = \mathbf{B}^H \mathbf{F}_N \mathbf{E}_n^H \mathbf{E}_n \mathbf{F}_N^{-1} \mathbf{B}$  is a symmetric and positive semidefinite  $N_{dr} \times N_{dr}$  matrix. By minimizing (10), the leaked power to the notch band used by the primary user is minimized.

### B. Code generator matrix design

As discussed in section II, the code generator matrix,  $\mathbf{G}$ , is designed to generate  $N_u$  zeros at the tail of the IDFT output. In addition to meeting this constraint, the code generator matrix can be designed to optimize the overall performance of the transmitter/receiver chain. In [14], the sum of the error variances at the output of two data estimators, namely the linear minimum mean squared error and best linear unbiased estimators, is considered to be minimized. By assuming the communication channel being AWGN, it is shown that a code generator matrix is optimum, regarding [14, relation (33)], if and only if  $\mathbf{G}$  satisfies

$$\mathbf{G}^H \mathbf{G} = \mathbf{I}, \quad (11)$$

and

$$\mathbf{F}_N^{-1} \mathbf{B} \mathbf{G} = \begin{bmatrix} * \\ \mathbf{0}_{N_u \times N_{dr}} \end{bmatrix}. \quad (12)$$

While keeping the above criteria as the bit error rate optimality criteria, we will add another condition on the code generator matrix, i.e. the minimization of the leaked sidelobes power to the notch band. Hence, the constrained optimization problem is defined as follows:

$$\min_{\mathbf{G}} P_n = \text{Tr}[\mathbf{G}^H \mathbf{A} \mathbf{G}] \quad (13)$$

$$\text{Subject to } \mathbf{G}^H \mathbf{G} = \mathbf{I}_{N_d} \quad (14)$$

$$\mathbf{F}_N^{-1} \mathbf{B} \mathbf{G} = \begin{bmatrix} * \\ \mathbf{0}_{N_u \times N_{dr}} \end{bmatrix}. \quad (15)$$

To solve the above problem, first, we rephrase the constraints in (15). Let  $\mathbf{Q} = [\mathbf{F}_N^{-1} \mathbf{B}]_{\text{last } N_u \text{ rows}}$  be the  $N_u \times N_{dr}$  matrix containing the last  $N_u$  rows of  $\mathbf{F}_N^{-1} \mathbf{B}$ . The second constraint can be rewritten as

$$\mathbf{Q} \mathbf{G} = \mathbf{0}_{N_u \times N_{dr}}. \quad (16)$$

To meet this constraint, we will use the following decomposition

$$\mathbf{G} = \mathbf{N}_Q \mathbf{C}, \quad (17)$$

where  $\mathbf{N}_Q = \text{Null}(\mathbf{Q}) \in \mathbb{C}^{N_{dr} \times (N_{dr} - N_u)}$  is the null space matrix of  $\mathbf{Q}$ , and the matrix  $\mathbf{C}$  with size  $(N_{dr} - N_u) \times N_d$  should be designed to suppress the sidelobes. By inserting (17) in (14), the first constraint can be expressed as follows:

$$\mathbf{G}^H \mathbf{G} = \mathbf{C}^H \mathbf{N}_Q^H \mathbf{N}_Q \mathbf{C} = \mathbf{C}^H \mathbf{C} = \mathbf{I}. \quad (18)$$

By replacing (17) and (18) in (13) and (14), the new optimization problem can be written as

$$\min_{\mathbf{C}} P_n = \text{Tr}[\mathbf{C}^H \mathbf{K} \mathbf{C}]$$

$$\text{Subject to } \mathbf{C}^H \mathbf{C} = \mathbf{I}_{N_d}, \quad (19)$$

where  $\mathbf{K} = \mathbf{N}_Q^H \mathbf{A} \mathbf{N}_Q$  is a symmetric positive semidefinite matrix. Note that the constraints (14) and (15) are replaced by a single orthogonality constraint in the new optimization problem. The above orthogonality constrained optimization problem is a classic problem which can be solved by using

one of the results of the Courant-Fisher minimax theorem [20]: For a given symmetric matrix (such as  $\mathbf{K}$ ) of dimension  $(N_{dr} - N_u) \times (N_{dr} - N_u)$  and an arbitrary unitary matrix  $\mathbf{C}$  of dimension  $(N_{dr} - N_u) \times N_d$  ( $N_d \leq (N_{dr} - N_u)$ ), the trace of  $\mathbf{C}^H \mathbf{K} \mathbf{C}$  reaches its minimum when  $\mathbf{C}$  is an orthogonal basis of the eigenspace of  $\mathbf{K}$  associated with the algebraically smallest eigenvalues. In particular, it is achieved for the eigen basis itself. If the eigenvalues are sorted in ascending order and  $\mathbf{U} = [\mathbf{u}_1, \dots, \mathbf{u}_{N_d}]$  are the eigenvectors associated with the first  $N_d$  eigenvalues  $\delta_1, \dots, \delta_{N_d}$  ( $\mathbf{U}^H \mathbf{U} = \mathbf{I}_{N_d}$ ), we have

$$\min_{\mathbf{C}} \text{Tr} [\mathbf{C}^H \mathbf{K} \mathbf{C}] = \text{Tr} [\mathbf{U}^H \mathbf{K} \mathbf{U}] = \delta_1 + \delta_2 + \dots + \delta_{N_d}. \quad (20)$$

This solution states that the minimized leaked power becomes the sum of the  $N_d$  smallest eigenvalues of  $\mathbf{K}$ . As a result, the minimized leaked power to the notch band is a function of the distribution of the eigenvalues of the matrix  $\mathbf{K}$  as well as the number of transmitted data symbols. This dependency will be discussed in the next section.

Note that the obtained code generator matrix is matched to the BLUE and to the LMMSE data estimators because it meets the optimality criteria in (14) and (15) which are proposed in [14]. Therefore, the proposed data estimators in [14] can be used at the receiver for the data estimation of the proposed UW-OFDM scheme in both the AWGN and frequency selective channels. Considering the implementation issues, as soon as the transmitter receives information on the spectral position of the primary system from the spectrum sensing unit, it forms the matrix  $\mathbf{E}_n$  as described to calculate the leaked power in (6). Then the matrices  $\mathbf{A}$  and  $\mathbf{K}$  are calculated. The last step is to decompose the matrix  $\mathbf{K}$  to its eigenvectors and select the suitable eigenvectors as the column vectors of the optimized code generator matrix. Note that once this code generator matrix is calculated, it can be used until primary users' spectrum changes. So, the implementation costs are the calculation of the matrices  $\mathbf{E}_n$ ,  $\mathbf{A}$  and  $\mathbf{K}$  and the eigenvalue decomposition of  $\mathbf{K}$ , which are performed only once after every spectral change of the primary users.

#### IV. NUMERICAL RESULTS

A non-systematic coded UW-OFDM system with  $N = 128$  subcarriers is considered. The number of redundant subcarriers is the same as the length of the UW which equals  $N_u = N_r = 16$ . The subcarrier interval is normalized to be  $\Delta f = 1$ . Without loss of generality, we have considered  $\mathbf{B} = \mathbf{I}_N$ . For plotting power spectra of all algorithms,  $10^4$  independent OFDM symbols are randomly generated, and the Welch method is used to calculate the power spectral density (PSD) of the transmitted signals. The simulations show that the model used for modeling the power spectral density of UW-OFDM in (5) fully matches the simulated PSD by the Welch method. So, only the simulated PSDs are shown in the figures. Unless otherwise stated, the PSDs are normalized.

For the first set of experiments, the notch band is assumed in the interval  $[20\Delta f, 40\Delta f]$  covering  $N_n = 21$  subcarriers. We denote the number of subcarriers available for data transmission to be  $N_d^* = N - N_z - N_r - N_n$  in which  $N_z$  is the

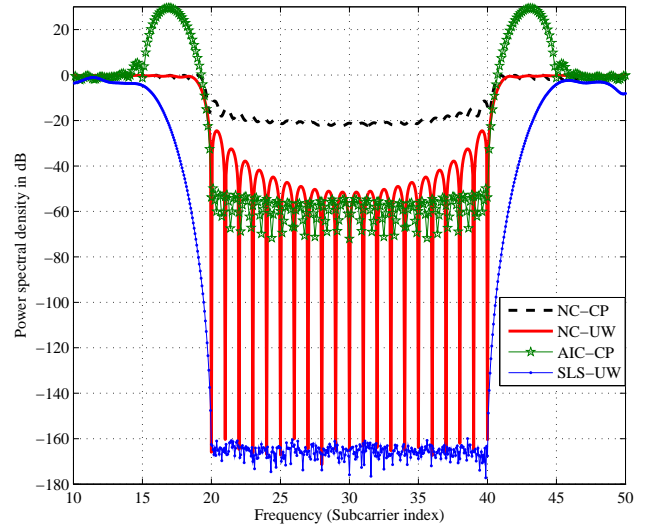


Fig. 1. The sidelobe suppression achieved by different approaches.

number of DC and edge band subcarriers, and  $N_n$  is the width of the notch band. So, in this example, we have  $N_d^* = 91$ . Fig. 1 shows the power spectrum of the proposed UW-OFDM system with sidelobe suppression (SLS-UW) at the notch band for  $N_d = 81 < N_d^*$ . It can be observed that the sidelobes are decreased to -160 dB, which is essentially zero, taking into account the numerical precision of the computing program. In comparison, the PSD of non-contiguous CP-OFDM (NC-CP), non-contiguous UW-OFDM (NC-UW) and CP-OFDM with the well-known AIC sidelobe suppression method (AIC-CP) are shown. In NC multicarrier techniques, the subcarriers in the notch band are simply turned off. For AIC-CP, four cancellation subcarriers are inserted at each side of the notch band, and the PSD is normalized to the peak value of the NC-CP method. The achieved sidelobe suppression of AIC-CP is 50 dB. However, it creates a spectrum overshoot of 30 dB on the cancellation carriers. This will reduce the available power for data transmission and degrades the BER performance. By just nulling the subcarriers in the notch band, NC-UW outperforms NC-CP, because the out-of-band radiation of UW-OFDM system is lower than CP-OFDM system [18]. It is noteworthy that in both CP-OFDM and UW-OFDM, the sharp transition between adjacent multicarrier symbols in time-domain increases the OOB power leakage. In CP-OFDM, time-domain pulse shaping is one of the most widespread approaches to ensure a smooth transition at the borders of the multicarrier symbols, and to also reduce the OOB radiation in practical implementations [21]. To consider the effect of the discussed sidelobe suppression technique only, no time-domain pulse shaping is considered for both UW-OFDM and CP-OFDM systems. It is clear that the time-domain pulse shaping technique can also be applied to UW-OFDM, further improving its sidelobe suppression performance.

As stated in the proposed solution of the sidelobe suppres-

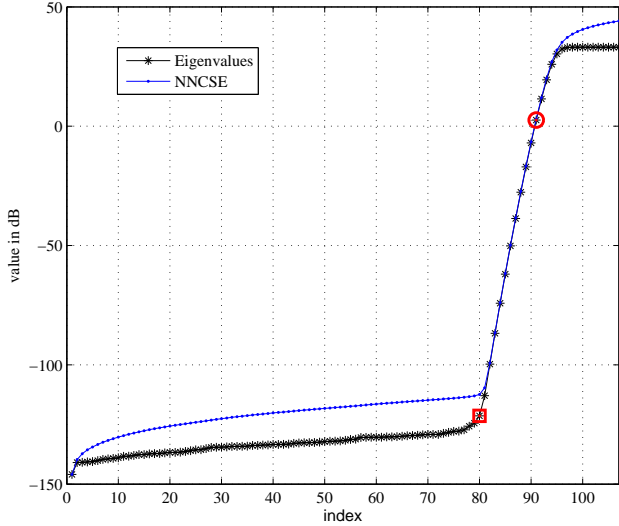


Fig. 2. The distribution and non-normalized cumulative sum of the eigenvalues for the matrix  $\mathbf{K}$ .

sion optimization problem in (20), the resulting leaked power of SLS-UW is the sum of the  $N_d$  smallest eigenvalues of the matrix  $\mathbf{K}$ . So, we define the non-normalized cumulative sum of the eigenvalues of  $\mathbf{K}$  as  $\text{NNCSE}(k) = \sum_{i=1}^k \delta_i$  for  $1 \leq k \leq N - N_z - N_u$ . The sidelobe suppression ability of SLS-UW can easily be characterized by the distribution and cumulative sum of the eigenvalues of  $\mathbf{K}$  which are shown in Fig. 2. As said, in this scenario, we have  $N_d^* = 91$ , which is emphasized by the circle marker. The first 81 smallest eigenvalues are essentially zero, after that the eigenvalues start to increase. Let us denote the eigenvalue index at which the NNCSE starts to increase as the threshold number of data symbols,  $N_d^{TH}$  for short, because this is the highest number of data symbols for which the strongest sidelobe suppression is achieved. So, by setting  $N_d \leq N_d^{TH} = 81$ , the ultimate sidelobe suppression is achieved. Note that  $N_d^{TH}$ , emphasized by the square marker in Fig. 2, is slightly lower than the allowed number of data symbols,  $N_d^*$ . The achieved sidelobe suppression for different number of transmitted data symbols is depicted in Fig. 3. The figure shows that for  $N_d \leq N_d^{TH} = 81$ , the sidelobes power is zero. For  $N_d^{TH} < N_d \leq N_d^* = 91$ , the sidelobe suppression is more than 50 dB, which is still good for many applications.

Simulation results not mentioned here for brevity show that the performance of SLS-UW almost does not depend on the relative place of the notch band in the whole spectrum. Moreover, SLS-UW is able to suppress the sidelobes in multiple non-contiguous spectral notch bands. We should only take care that all non-contiguous notch bands are included in the matrix  $\mathbf{E}_n$  in (6). An interesting behavior of the proposed SLS-UW is that when the width of the notch band increases, its sidelobe suppression performance improves. This behavior is investigated in Fig. 4 in which different notch band widths of  $\{13, 25, 37, 49, 61\}$  are simulated. The number of data symbols

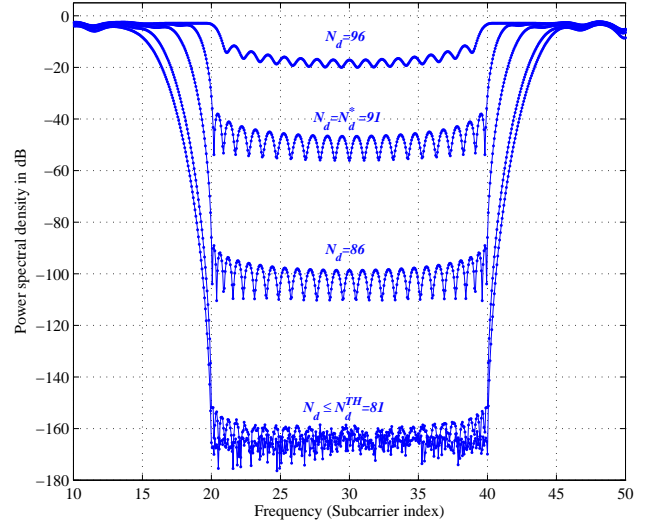


Fig. 3. The achieved sidelobe suppression by SLS-UW-OFDM system with different number of data symbols ( $N_d$ ).

is assumed to be the maximum allowed value of  $N_d^*$  for each case. In this figure, the width of the notch band is increased with a fixed amount of carriers, and it is observed that at the same time, the achieved sidelobe suppression is increased with a fixed amount. This is further investigated by plotting the distribution of the eigenvalues of  $\mathbf{K}$  for the different cases in Fig. 5. The eigenvalues of the smallest notch band are illustrated in the right-most starred curve. The value of the eigenvalue with the index  $N_d^*$  is indicated by the circle marker. This value decreases when the notch band width increases. Therefore, when the width of the notch band increases, the difference between the value of  $N_d^*$  and  $N_d^{TH}$  decreases which means that the throughput loss for having zero sidelobes decreases.

## V. CONCLUSION

One of the main challenges of deploying multicarrier techniques to use the non-contiguous available spectrum holes in cognitive radio networks is the high sidelobes power. In this paper, a novel sidelobe suppression technique is proposed for the non-systematic coded UW-OFDM system. The sidelobe suppression is achieved by designing the code generator matrix without the need for any extra processing, which is in contrast to most of the sidelobe suppression methods proposed for the CP-OFDM system. We have shown how a trade-off can be achieved between the system throughput and sidelobe suppression: by sacrificing a few subcarriers, the sidelobe power is reduced significantly. By setting the number of transmitted data symbols below a threshold, typically resulting in only a slight decrease in the system throughput, an outstanding zero sidelobes power can be obtained.

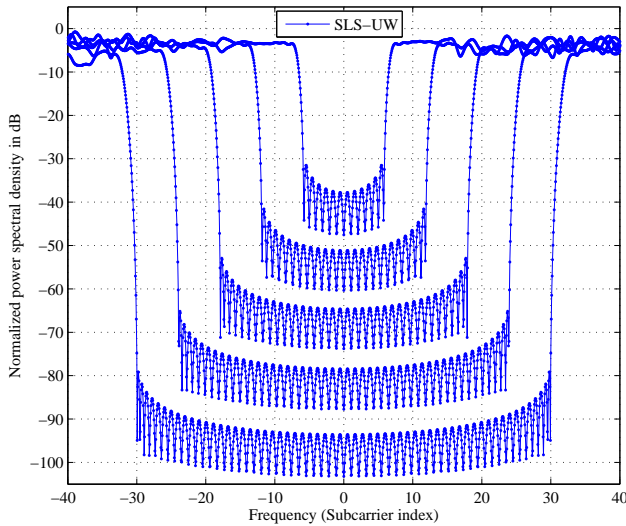


Fig. 4. The achieved sidelobe suppression by SLS-UW-OFDM system with different notch widths of  $\{13, 25, 37, 49, 61\}$  when  $N_d = N_d^*$ .

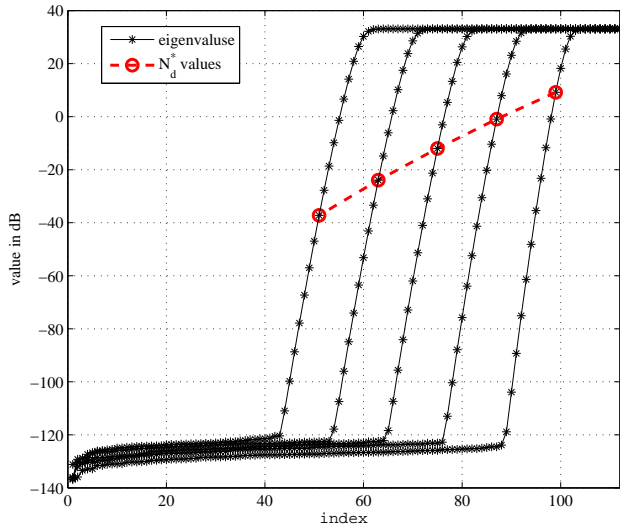


Fig. 5. The distribution of the eigenvalues for different notch widths and  $N_d = N_d^*$ .

#### ACKNOWLEDGMENT

This research has been funded by the Interuniversity Attraction Poles Programme initiated by the Belgian Science Policy Office.

#### REFERENCES

[1] FCC, *Spectrum policy task force report, ET Docket No. 02-135*, Nov. 2002., Std.  
 [2] S. Haykin, "Cognitive radio: brain-empowered wireless communications," *Selected Areas in Communications, IEEE Journal on*, vol. 23, no. 2, pp. 201–220, Feb. 2005.

[3] H. Mahmoud, T. Yucek, and H. Arslan, "OFDM for cognitive radio: merits and challenges," *Wireless Communications, IEEE*, vol. 16, no. 2, pp. 6–15, 2009.  
 [4] D. Qu, Z. Wang, and T. Jiang, "Extended active interference cancellation for sidelobe suppression in cognitive radio OFDM systems with cyclic prefix," *Vehicular Technology, IEEE Transactions on*, vol. 59, no. 4, pp. 1689–1695, 2010.  
 [5] S. Brandes, I. Cosovic, and M. Schnell, "Reduction of out-of-band radiation in OFDM systems by insertion of cancellation carriers," *Communications Letters, IEEE*, vol. 10, no. 6, pp. 420–422, 2006.  
 [6] H. Mahmoud and H. Arslan, "Sidelobe suppression in OFDM-based spectrum sharing systems using adaptive symbol transition," *Communications Letters, IEEE*, vol. 12, no. 2, pp. 133–135, Feb. 2008.  
 [7] S. Pagadarai, R. Rajbanshi, A. M. Wyglinski, and G. Minden, "Sidelobe suppression for OFDM-based cognitive radios using constellation expansion," in *Wireless Communications and Networking Conference, 2008*, April 2008, pp. 888–893.  
 [8] Y. Zhou and T. Jiang, "Active point modification for sidelobe suppression with papr constraint in OFDM systems," *Wireless Networks*, pp. 1–11, 2013. [Online]. Available: <http://dx.doi.org/10.1007/s11276-013-0561-5>  
 [9] X. Zhou, G. Li, and G. Sun, "Low-complexity spectrum shaping for OFDM-based cognitive radio systems," *Signal Processing Letters, IEEE*, vol. 19, no. 10, pp. 667–670, Oct. 2012.  
 [10] H.-M. Chen, W.-C. Chen, and C.-D. Chung, "Spectrally precoded OFDM and OFDMA with cyclic prefix and unconstrained guard ratios," *Wireless Communications, IEEE Transactions on*, vol. 10, no. 5, pp. 1416–1427, May 2010.  
 [11] J. van de Beek, "Sculpting the multicarrier spectrum: a novel projection precoder," *Communications Letters, IEEE*, vol. 13, no. 12, pp. 881–883, December 2009.  
 [12] A. Tom, A. Sahin, and H. Arslan, "Mask compliant precoder for OFDM spectrum shaping," *Communications Letters, IEEE*, vol. 17, no. 3, pp. 447–450, March 2013.  
 [13] A. Onic and M. Huemer, "Direct vs. two-step approach for unique word generation in UW-OFDM," in *International OFDM Workshop, 2010*, pp. 285–299.  
 [14] M. Huemer, C. Hofbauer, and J. Huber, "Non-systematic complex number RS coded OFDM by unique word prefix," *Signal Processing, IEEE Transactions on*, vol. 60, no. 1, pp. 285–299, Jan. 2012.  
 [15] C. Hofbauer and M. Huemer, "A study of data rate equivalent UW-OFDM and CP-OFDM concepts," in *IEEE ASILOMAR, 2012*, pp. 173–177.  
 [16] M. Huemer, A. Onic, and C. Hofbauer, "Classical and bayesian linear data estimators for unique word OFDM," *Signal Processing, IEEE Transactions on*, vol. 59, no. 12, pp. 6073–6085, 2011.  
 [17] C. Hofbauer, M. Huemer, and J. Huber, "On the impact of redundant subcarrier energy optimization in UW-OFDM," in *Signal Processing and Communication Systems (ICSPCS), 2010 4th International Conference on*, 2010, pp. 1–6.  
 [18] M. Rajabzadeh, H. Steendam, and H. Khoshbin, "Power spectrum characterization of systematic coded UW-OFDM systems," in *Vehicular Technology Conference (VTC Fall), 2013 IEEE 78th*, 2013, pp. 1–5.  
 [19] H. Steendam, "On the selection of the redundant carrier positions in UW-OFDM," *Signal Processing, IEEE Transactions on*, vol. 61, no. 5, pp. 1112–1120, March 2013.  
 [20] B. N. Parlett, *The symmetric eigenvalue problem*. SIAM, 1980, vol. 7.  
 [21] B. Farhang-Boroujeny and R. Kemper, "Multicarrier communication techniques for spectrum sensing and communication in cognitive radios," *Communications Magazine, IEEE*, vol. 46, no. 4, pp. 80–85, 2008.